
Numerical Modelling of Twisted Nematic Devices

D. W. Berreman

Phil. Trans. R. Soc. Lond. A 1983 **309**, 203-216

doi: 10.1098/rsta.1983.0034

Email alerting service

Receive free email alerts when new articles cite this article - sign up in the box at the top right-hand corner of the article or click [here](#)

To subscribe to *Phil. Trans. R. Soc. Lond. A* go to: <http://rsta.royalsocietypublishing.org/subscriptions>

Numerical modelling of twisted nematic devices

BY D. W. BERREMAN

Bell Laboratories, 600 Mountain Avenue, Murray Hill, New Jersey 07974, U.S.A.

Over most of each active region in nematic and chiral nematic twist cells the motion and configuration of the liquid crystal layer does not vary appreciably with position parallel to the surfaces. In such laminar regions the statics, dynamics and optics of the cell can be accurately simulated at low cost on a computer of moderate size, given the appropriate physical parameters. Methods and recent advances in simulation of laminar regions are reviewed. Bistable twist cells are simulated for illustration. Important problems of stability and edge effects in the presence of electric fields await solution with two- or three-dimensional simulations.

INTRODUCTION

In recent years many laboratories have set up computer programs to simulate the behaviour of nematic and chiral nematic displays. Several of these laboratories have published results of investigations into the effects of varying parameters on the static optical performance of twist cells (Baur 1980, 1981; van Doorn *et al.* 1980; Birecki & Kahn 1980). Simulation of dynamic behaviour has also been done and has led to an understanding of reverse-twist and optical bounce effects (van Doorn 1975; Berreman 1975*a*). Interesting effects from 'weak anchoring' of directors on cell surfaces have been predicted by such computer simulation (Berreman 1980) but they remain largely unrealized (Yang 1983).

Twist cells with very high multiplexing numbers are used in some modern hand-held calculators. Computer simulation shows how parameters may be optimized to achieve such high multiplexing numbers (Baur 1980, 1981; van Doorn *et al.* 1980; Birecki & Kahn 1980).

We are currently interested in bistable chiral nematic twist cells (Heffner & Berreman 1982; Berreman & Heffner 1982). Successful computer simulation of their static, dynamic and optical behaviour has greatly enhanced our understanding of the operation of these cells. The first dynamic simulation of a bistable twist cell was done before one was made.

Many twist cells are made with chiral dopants in an ordinary nematic liquid crystal. Our experience suggests that the dopant concentration is usually low enough for the elastic, dielectric and optical parameters to be close to those of the nematic host. However, the usual methods of measuring these parameters are not applicable when the material is chiral. A comparison of static measurements of the optical behaviour or capacitance in twist cells with computer predictions would provide a means for measuring elastic, dielectric and optical parameters of chiral mixtures.

MODELLING CELLS WITH ONE-DIMENSIONAL VARIATION OF DIRECTORS

Computer simulation of twist cell behaviour is done in two stages. First the orientation of the nematic director as a function of distance from each cell surface is computed with a particular set of parameters. For equilibrium states the required parameters are the mean-square electric displacement field, the two dielectric and three elastic constants and the natural helicity, if the nematic is chiral, and the orientation of the director at each surface. The electrical capacitance

[133]

per unit area in the cell is a useful by-product of this computation of director orientation. The mean-square voltage is determined by the displacement and the capacitance. It is also easy to integrate the components of the energy density to obtain the energies per unit area in the cell.

Once the director configuration is found, the optical transmission and reflexion may be computed as a function of wavelength and viewing direction. This requires knowledge of the anisotropic optical parameters of the liquid crystal. Guest–host displays may easily be simulated by using complex numbers for the optical parameters to include absorption. Polarizers, conductive coatings, glass and even a reflective layer may be included in the sandwich for optical computations. So long as scattering is negligible, these computations may be done quickly on a computer by using a 4×4 matrix method (Smith 1965; Berreman & Scheffer 1970). Scattering must be treated separately.

To compute dynamic effects an initial configuration, which may come from an equilibrium computation, and five viscosity parameters are needed in addition to the previously listed parameters. There are very few liquid crystals for which the five viscosities have been determined. However, comparisons of observed dynamic variation of optical transmission or cell capacitance with predictions from fluid dynamic computations are possible and would provide a means for determining or verifying estimates of these viscosities.

There are two classes of numerical methods for finding director configurations in regions where variation parallel to the surfaces is negligible. One class is based on direct integration of the Euler–Lagrange differential equations for minimum Helmholtz free-energy per unit area in the liquid crystal. In this case the director orientation and its rate of change with z position is estimated at one point, such as one surface. The differential equations are then integrated to the opposite surface by a numerical method. If the integration does not give the desired orientation at the second surface, the initial conditions are altered, within the restrictions set by the problem, until it does.

The second is the class of relaxation methods. This class may include the full dynamic problem or it may be abbreviated by ignoring transverse motion of the fluid. In these computations an initial configuration is assigned to the directors and the configuration is then adjusted according to certain equations of motion that cause the energy in the liquid crystal to relax toward a minimum.

INTEGRATING STATIC EULER–LAGRANGE EQUATIONS

The strain free-energy density of a chiral nematic liquid crystal is described by the Oseen–Frank equation (Oseen 1933; Frank 1958; de Gennes 1975). When the director varies only in the z direction, normal to the surface, this free energy may be written as follows in Cartesian and polar coordinates:

$$\begin{aligned} F_s &= \frac{1}{2}k_{11}(n'_z)^2 + \frac{1}{2}k_{22}(n_x n'_y - n_y n'_x - 2\pi/P)^2 + \frac{1}{2}k_{33}\{(n_z n'_x)^2 + (n_z n'_y)^2 + (n_x n'_x + n_y n'_y)^2\} \\ &= \frac{1}{2}k_{11}(\theta' \sin \theta)^2 + \frac{1}{2}k_{22}(\beta' \sin^2 \theta - 2\pi/P)^2 + \frac{1}{2}k_{33} \cos^2 \theta \{\theta'^2 + (\beta' \sin \theta)^2\}. \end{aligned}$$

k_{ii} are elastic coefficients, n_i are rectangular director components and P is the 360° pitch of the unstrained chiral nematic. The angle β is the azimuth and θ is the tilt measured from normal to the surfaces. Primes represent differentials with respect to z . The electrostatic free-energy density is

$$\begin{aligned} F_e &= \frac{D^2}{2\epsilon_0\{\epsilon_{\parallel} n_z^2 + \epsilon_{\perp}(n_x^2 + n_y^2)\}} \\ &= \frac{D^2}{2\epsilon_0(\epsilon_{\parallel} \cos^2 \theta + \epsilon_{\perp} \sin^2 \theta)}, \end{aligned}$$

where D is the displacement field and ϵ_{\perp} is the degenerate component of the dielectric tensor. The Helmholtz free-energy density is the strain free-energy plus the electrostatic free-energy: $F_H = F_s + F_e$. Equilibrium configurations are such that the integral of the Helmholtz free-energy density from one surface to the other has an extreme value, subject to the conditions imposed at the boundaries (see, for example, Thurston & Berreman 1981).

The Gibbs free-energy density is the strain free-energy density minus the electrostatic energy density. The integral, G , of the Gibbs free-energy with fixed applied voltage is also extremal (see, for example, Thurston & Berreman 1981). However, since it is necessary to know the configuration before the local voltage gradient can be defined, this fact is not useful in finding configurations.

The Euler–Lagrange equations to obtain extremal integrals of the Helmholtz free-energy are least complicated in polar coordinates. They are

$$\frac{\partial F_H}{\partial \theta} - \frac{d}{dz} \left(\frac{\partial F_H}{\partial \theta'} \right) = 0,$$

and, because F_H does not depend explicitly on β ,

$$\partial F_H / \partial \beta' = T,$$

where T is a constant of integration and is also a measure of torque about the polar axis.

The preceding Euler–Lagrange equations may be manipulated to give

$$\theta'' = \left(\frac{\sin \theta \cos \theta}{k_{11} \sin^2 \theta + k_{33} \cos^2 \theta} \right) \left\{ (k_{33} - k_{11}) \theta'^2 + 2k_{22} \beta' (\beta' \sin^2 \theta - 2\pi/P) \right. \\ \left. + k_{33} \beta'^2 (\cos^2 \theta - \sin^2 \theta) + \frac{D^2 (\epsilon_{\parallel} - \epsilon_{\perp})}{\epsilon_0 (\epsilon_{\parallel} \cos^2 \theta + \epsilon_{\perp} \sin^2 \theta)^2} \right\}$$

and

$$\beta' = \frac{T / \sin^2 \theta + k_{22} 2\pi/P}{k_{22} \sin^2 \theta + k_{33} \cos^2 \theta}.$$

These equations combine appropriate parts from the Leslie equations (Leslie 1970) for chiral nematics in magnetic fields and the Deuling equations (Deuling 1974) for twisted ordinary nematics in electric fields.

A disadvantage of polar coordinates is that special care must be taken if the director comes close to parallel with the polar axis, $\theta = 0$. The difficulty is with the second, β' equation, which gives a divergent value at $\theta = 0$ unless the torque, T , is zero. Fortunately θ will be exactly zero only at the surfaces, if at all, in non-trivial static problems. In that case it is known in advance that no torque can be maintained and the integration actually becomes simpler. When θ only comes close to zero we maintain accuracy in the integration by shortening the steps so that the change in β per step does not exceed a few degrees.

HUNTING FOR STATIC CONFIGURATIONS

Once a routine for integrating the equations for director configuration is written it is still necessary to provide an efficient means to estimate the initial conditions necessary to obtain a solution consistent with the desired boundary conditions. This will be illustrated by an example. Suppose we are considering a chiral nematic cell with directors attached parallel to the surface at one surface ($\theta_i = 90^\circ$) and at an angle $\theta_f = 55^\circ$ at the other. Suppose further that the director at the second surface is turned $\frac{3}{4}$ turn with respect to the first ($\beta_f = 270^\circ$). Let the elastic constants and dielectric constants be those for E7, as listed in table 1. Let us find a configuration at 1.43 V.

(In our program we actually aim towards $V^2 = 2.045$.) Before we can start the integration we must estimate the rates of change of θ and β at the first surface and also the displacement field. (In practice we estimate θ' , $\beta' \sin \theta$ and D^2 because the final results vary more smoothly with these functions when θ or D is small.)

TABLE 1. ASSUMED PARAMETERS FOR CHIRAL DOPED E7 NEMATIC MIXTURE AT 20 °C

splay, twist and bend elastic constants (Raynes *et al.* 1979)

$$k_{11} = 11.7 \times 10^{-12} \text{ N} \quad k_{22} = 8.8 \times 10^{-12} \text{ N} \quad k_{33} = 19.5 \times 10^{-12} \text{ N}$$

extraordinary and ordinary dielectric constants (Raynes *et al.* 1979)

$$\epsilon_{\parallel} = 19.5 \quad \epsilon_{\perp} = 5.17$$

viscosity parameters (twice those for MBBA) (de Jeu 1978)

$$\gamma_1 = 0.190 \text{ Pa s} \quad \eta_1 = 0.242 \text{ Pa s} \quad \eta_2 = 0.0476 \text{ Pa s} \quad \eta_3 = 0.0832 \text{ Pa s} \quad \eta_{12} = 0.0130 \text{ Pa s}$$

optical parameters for 0.6328 μm light

$$n_o = 1.513 \quad n_e = 1.728$$

After a few guesses we can find four different tries that lead to approximately the desired configuration, as illustrated in figure 1. Then we assume that the final results are approximately linearly dependent on the initial estimates:

$$\theta_f \approx a_{11} + a_{12} D^2 + a_{13} \theta' + a_{14} \beta' \sin \theta,$$

$$\beta_f \approx a_{21} + a_{22} D^2 + a_{23} \theta' + a_{24} \beta' \sin \theta,$$

and

$$V^2 \approx a_{31} + a_{32} D^2 + a_{33} \theta' + a_{34} \beta' \sin \theta.$$

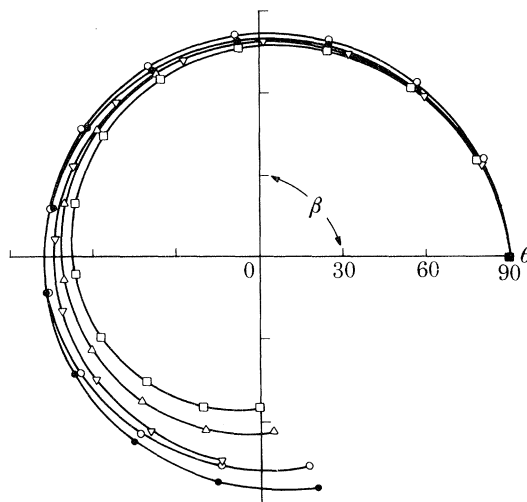


FIGURE 1. Search for a configuration at 1.43 V in an asymmetric cell with $\theta_i = 90^\circ$, $\theta_f = 55^\circ$, $\beta_f = 270^\circ$, thickness: pitch ratio $h/P = 0.5$. Hunting is done by fixing θ_i and adjusting θ' , $\beta' \sin \theta$ and D^2 . Liquid crystal parameters are given in table 1. Marks are at equally spaced levels in the cell.

With the four tries we obtain four sets of parameters for these three approximate equations, enough to determine the 12 values of a_{ij} . We may then invert the equations and get a linear estimate of the initial conditions that would give the desired values of θ_f , β_f and V^2 . The actual integration with the newly found initial parameters will miss the mark slightly but the process may be repeated, replacing a poor estimate with the newest one. Five or six iterations of this procedure, which is easily automated, usually gives the desired results of the integration to one part in 10000.

Once one solution is found it is only necessary to use four of the previous approximate solutions and alter the target value of V^2 to find another solution nearby. This process can be continued to get the variation of solutions with V^2 without much further human intervention.

If plots of various functions against V are to be made, it is often unnecessary to seek solutions at a particular value of V . In those cases we select a series of values of D^2 , use only three trial solutions and the first two of the three preceding equations with a_{i2} omitted and let the computed values of V fall where they may. This procedure avoids a problem that arises if there are multiple solutions at a single voltage, since the solutions are usually monotonic functions of D^2 .

SPECIAL TREATMENT FOR SYMMETRICAL CELLS

In cells that have the same director tilt at each surface, configurations at moderate voltages are usually symmetrical about the mid-plane. At the mid-plane either $\theta = 90^\circ$ or $\theta' = 0$, and β is half its final value. It is useful to start the integration at the centre of the cell to find such solutions because the trajectories are less sensitive to small errors in launching parameters there. If θ' is zero, we adjust the initial value of θ rather than θ' but otherwise the procedure is the same as if we started at one surface. Such a search is illustrated in figure 2, for a cell with $\beta_t = 360^\circ$ and surface tilts of 55° .

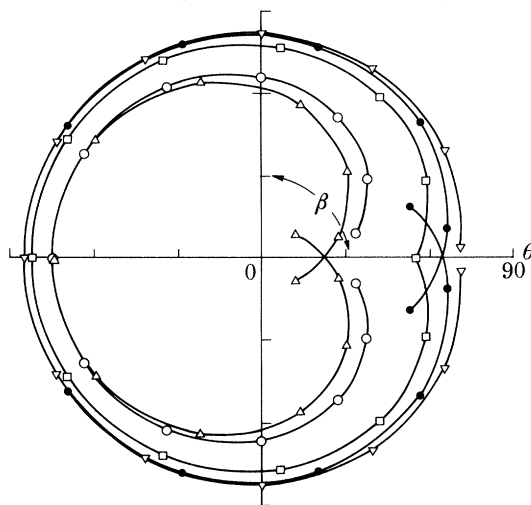


FIGURE 2. Search for configuration at 1.86 V in a symmetric twist cell with boundary tilts $\theta_1 = \theta_2 = 55^\circ$, $\beta_t = 360^\circ$, and $h/P = 1$. Hunting was done by using $\theta' = 0$ at the mid-plane and adjusting θ , $\beta' \sin \theta$ and D^2 . Liquid crystal parameters are from table 1.

There is also one analytic solution to the trajectory equations in symmetrical cells that may be used as a starting configuration in place of one found by trial and error. This configuration is one of constant tilt θ and constant β' . Hence

$$\beta' = (\beta_t - \beta_1)/h$$

and the first Euler-Lagrange equation in polar coordinates may be solved for D^2 , giving

$$D^2 = \left\{ \frac{\epsilon_0 (\epsilon_{\parallel} \cos^2 \theta + \epsilon_{\perp} \sin^2 \theta)^2}{(\epsilon_{\parallel} - \epsilon_{\perp})} \right\} \beta' \{ 2k_{22} (2\pi/P - \beta' \sin^2 \theta) + k_{33} \beta' (\sin^2 \theta - \cos^2 \theta) \}.$$

Even if D^2 computed from the preceding equation is negative so that D is imaginary, the solutions may still be continued into the physically meaningful region. The voltage on the cell is

$$V = \frac{hD}{\epsilon_0(\epsilon_{\parallel} \cos^2 \theta + \epsilon_{\perp} \sin^2 \theta)}.$$

USING STATIC CONFIGURATION RESULTS

To illustrate the usefulness of static configuration computations I shall carry through with more computations on the two cells considered in the preceding section.

It is often very instructive to make plots of Gibbs free-energy in the cell as a function of the square of the applied voltage (see figures 3 and 4). At zero voltage the plot is a line of nearly constant slope. The slope depends on the capacitance of the cell when in its field-free configuration. The curve then passes through a region of transition and finally follows another line of nearly constant slope that depends on the capacitance when the directors are mostly aligned nearly parallel to the electric field, if the liquid crystal has positive dielectric anisotropy, or perpendicular to it if the anisotropy is negative. In cells with high multiplexing numbers the change in slope is very abrupt. In bistable cells such curves double back to make a loop as illustrated in figures 3 and 4. The top of the loop is formed by unstable equilibrium states that are higher in energy than two adjacent bistable states at the same voltage, one of which is on the steeper and one on the gentler sloping line.

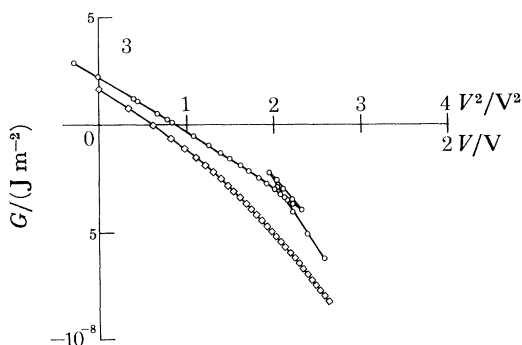


FIGURE 3. Gibbs free-energy plotted against V (nonlinear bottom scale) and V^2 (linear top scale) for the cell in figure 1 if it is $10 \mu\text{m}$ thick. Notice that the topologically separate states (\diamond) with 90° twist have lower energy than the bistable states (\circ) for this configuration. If they can be initiated, the bistable configurations eventually decay through disclination lines to this 90° twist state.

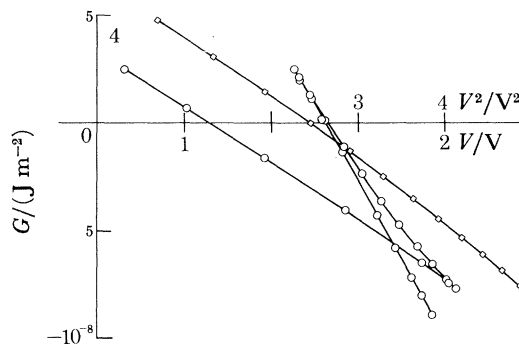


FIGURE 4. Gibbs free-energy plotted against V^2 for cell described in figure 2 if it is $10 \mu\text{m}$ thick. \diamond , A topologically separate set of states with final $\beta = 180^\circ$, invariant mid-plane tilt 90° and final tilt 125° , which could be reached by the same cell through a disclination line if it were energetically preferred.

Because of the ambiguity in direction of a director, one should always investigate solutions that differ from the expected one by half a turn, and that have a final tilt that is the supplement of the expected value, as shown at the right in figure 7. Such alternative solutions are not accessible from the others through continuous director motion that is invariant parallel to the surfaces. However, they may form through the passage of a disclination line across the picture element. This will occur if the alternative solution has a lower energy than the intended ones, as in figure 3. If the undesired state is lower in energy only briefly during switching of the cell, it may

not have sufficient time to develop. Nevertheless it is desirable to avoid such possibilities altogether since transitions through disclinations are usually slow to reverse.

Another curve that is instructive is a plot of the director tilt angle at the centre of the cell as a function of applied V^2 . In the usual twist cell of positive dielectric anisotropy this angle (measured from normal to the surfaces) will approach zero as the voltage increases. In a cell with high

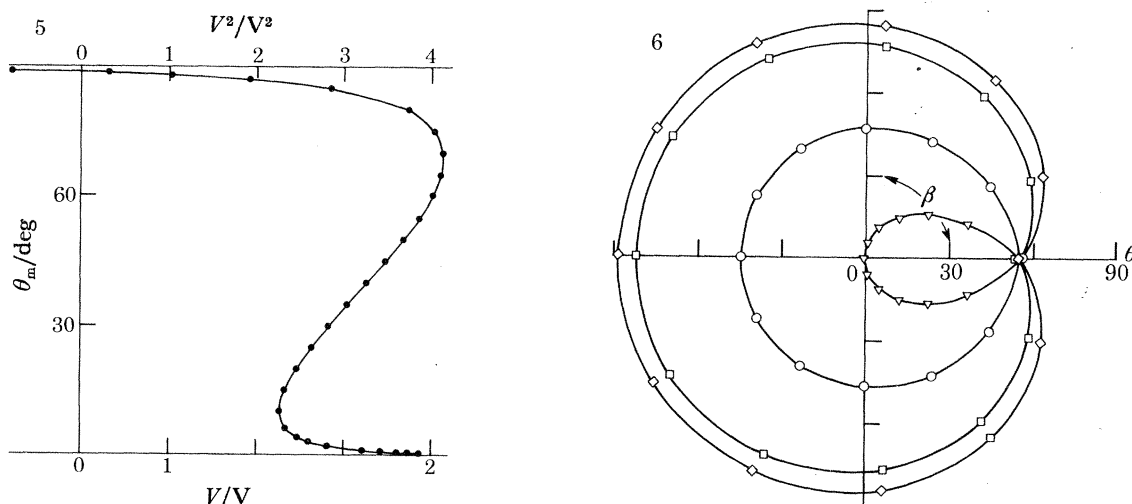


FIGURE 5. Mid-plane tilt θ_m plotted against V^2 (linear top scale) and V (bottom scale). Data from the four configurations of the preceding figure are included. The cell is bistable between about 1.5 and 2.1 V if nothing nucleates a transition to the state of lower energy through a moving 'wall'.

FIGURE 6. Three configurations at 1.86 V and one at no field (\diamond). The inner (first) and third loops are stable; the intermediate one is unstable. The first loop is the UP state; the third the DOWN state. Parameters are as in the previous figure. The outermost loop is the only stable solution at no field with 360° twist.

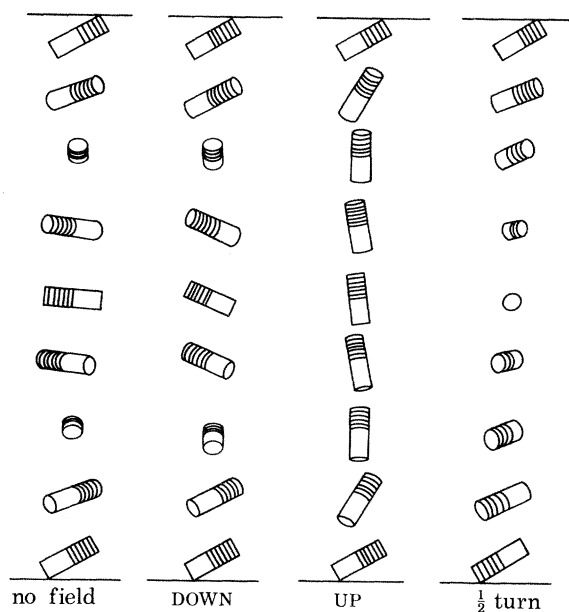


FIGURE 7. Illustration of director configurations for the three stable states of figure 6 and an alternative half-turn state. DOWN designates the state at 1.86 V with directors most nearly parallel to the surfaces, and UP that with directors most nearly normal. Tilt near the centre in the UP state is exaggerated.

multiplexing numbers the angle will change very abruptly when some optimal operating voltage is reached. In a bistable cell this effect is exaggerated and the curve doubles back on itself, with the region of positive slope representing the unstable states between the stable ones. Such a curve is shown in figure 5 for the cell with 360° azimuth change. Similar effects in non-chiral nematics have been studied by Scheffer (1980) and Thurston (1982).

Plots of the configuration of the cell close to the operating voltage are useful in estimating the optical properties of the cell. The data used to plot the configuration may be used in an optics program to compute the optical properties in detail if an estimate is insufficient. Figure 6 shows the configurations of two stable states and the intermediate unstable state of the same bistable cell at 1.86 V. The outermost loop on the figure is the configuration of the cell with no applied field. The optical properties of the state with no field are very similar to those of the outermost of the bistable states because the director configuration is nearly the same. Figure 7 shows the three stable configurations of figure 6 pictorially, together with the alternative half-turn state.

LAMINAR FLUID DYNAMICS

In dynamic problems there is frequently a point where the director passes through the direction normal to the surfaces. The problem of evaluating β' in that case cannot be disposed of easily as for static solutions. In 1975 descriptions of two somewhat different ways to do computer simulation of twist cell dynamics, ignoring effects of momentum and compressibility, were published (van Doorn 1975; Berreman 1975*a*). Van Doorn set up the Leslie–Ericksen torque equations (Ericksen 1961; Leslie 1968; Aslaksen 1971[†]) and used polar coordinates to describe director orientation when the director was not too nearly parallel to the polar axis. He used x - and y -components of the rectangular coordinates and a Lagrange multiplier when the director was close to the poles. The author used a non-orthogonal curved-net coordinate system that was limited in range mainly to the upper hemisphere. We have since taken van Doorn's idea of using rectangular coordinates and a Lagrange multiplier, but have done so in such a way that the multiplier is never explicitly evaluated, and the three coordinates appear on an equal footing in the equations. This method avoids changing coordinate systems and it also avoids limitations in range of rotation.

Shear flow complicates the problem but the method can be illustrated by considering only viscous resistance to local rotation. In that case the equations may be derived by using the same Helmholtz free-energy as in the statics problem and a Rayleigh dissipation function (see, for example, Goldstein 1950) defined by the expression

$$F_d = \frac{1}{2}\gamma_1(\dot{n}_x^2 + \dot{n}_y^2 + \dot{n}_z^2).$$

A generalized Lagrangian function (neglecting kinetic energy) that allows the use of three Cartesian director components while restricting the director to fixed length is

$$L = -F_H - \frac{1}{2}\lambda(n_x^2 + n_y^2 + n_z^2),$$

where λ is a Lagrange multiplier on the expression for the square of the constant director length. The equations of motion are

$$\frac{\partial L}{\partial n_i} - \frac{d}{dz} \left(\frac{\partial L}{\partial \dot{n}_i} \right) + \frac{\partial F_d}{\partial \dot{n}_i} = 0.$$

[†] In Aslaksen (1971), \sin should be replaced by \cos in the middle of the matrix in equation (1.10), and r by $-r$ in equation (2.7).

When expanded, these three ‘torque equations’ have the form

$$Q_i + \lambda n_i = \gamma_1 \dot{n}_i.$$

The Lagrange multiplier may be eliminated by the following method. Multiply each of these three equations by the corresponding director component n_i and sum them to obtain

$$\sum Q_i n_i + \lambda \sum n_i^2 = \gamma_1 \sum n_i \dot{n}_i.$$

Then notice that $\sum n_i^2 = 1$ so that $\sum n_i \dot{n}_i = 0$. Hence

$$\lambda = - \sum Q_i n_i.$$

This expression for λ may be inserted in the three torque equations, which can finally be rewritten as

$$Q_i(n_j^2 + n_k^2) - n_i(n_j Q_j + n_k Q_k) = \gamma_1 \dot{n}_i.$$

The moving directors computed from these equations maintain unit total length to first order, but it is still necessary to avoid slow deviation by renormalizing them to unity at least occasionally. We do so after each step in time.

The equations just obtained will give the correct equilibrium configurations if allowed to run for a long time. Because shear flow and forces are ignored, the computed dynamic behaviour is somewhat slower than and different from the actual behaviour. However, the computations are faster than those that include flow. A version of this simplified relaxation method was used to find approximate dynamic and static equilibrium configurations (Baur *et al.* 1975) before we wrote the static configuration program.

We have not found a general Rayleigh dissipation function to describe shear flow. Instead we use two shear-force and three torque equations derived from the Leslie–Ericksen equations (Berreman 1975 *a*; Aslaksen 1971) when we include shear. We use the substitutions just described to subject the directors to the unit-length constraint without explicitly introducing the Lagrange multiplier into the three torque equations. The forms of the two shear equations are

$$\sigma_{zx} = R_{11} V'_x + R_{12} V'_y + \sum S_{1i} n_i$$

and

$$\sigma_{zy} = R_{21} V'_x + R_{22} V'_y + \sum S_{2i} n_i,$$

where V'_i is a component of shear velocity gradient. The spatially invariant shear force σ is adjusted to make the integral of V' equal zero in twist cells, or the relative velocity of the surfaces in shear experiments. The form of the three torque equations is

$$Q_i(n_j^2 + n_k^2) - n_i(n_j Q_j + n_k Q_k) = T_{i1} V'_x + T_{i2} V'_y + \gamma_1 \dot{n}_i.$$

The expansion of the terms Q , R , S and T in these five equations is lengthy but it may be inferred by referring to the detailed expansion into four equations in polar coordinates in Berreman (1975 *a*), where R , S and T were all included in T_{ij} and Q was represented by λ .

Ultimately the expressions for time derivatives of the directors are functions of the directors and their first and second derivatives with respect to z . To approximate the derivatives, some scheme that is equivalent to fitting a ‘spline’ curve through the level z in question and its near neighbours is used. The simplest spline is a parabola for each component of the director at one level, fitted at that level and its two nearest neighbours. Computations with this spline are fast and stable most of the time. However, when torques are dominated by shear flow the progress becomes weakly unstable, resulting in slow growth of a ‘zig-zag’ pattern in the director as a function of z . This

instability is not changed by shortening the time steps. This effect can be avoided by smoothing the components once every 20 or 30 time steps with a spline consisting of a parabola fitted by least-squares among the five levels with two on each side of the adjusted level. When there is no such zig-zag instability, smoothing in this way proves to have almost no effect either on the equilibrium configurations or on the rate of flow or configuration change, even when it is done at every step. Once the zig-zag pattern is smoothed it seldom regains an appreciable amplitude in half a cycle of the operation of a twist cell. Even if the zig-zag pattern is uncontrolled it ultimately shrinks when the configuration nears the equilibrium curve, as shown in figure 8.

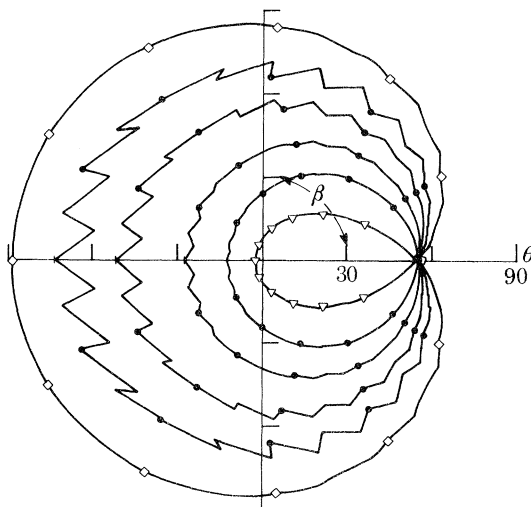


FIGURE 8. Second, field-free, half of a twist-cell cycle showing growing zig-zag pattern when smoothing is omitted. See figures 9 and 10 for other details, except that field remains off for 0.2 s for the outer loop in this figure.

All of the splines mentioned are simply weighted sums of each Cartesian component at the level in question and at one or two neighbours on either side. The weights needed to obtain the smoothed component and the first and second derivatives depend only on the distances to the neighbours. All these weights are computed at the start and stored in arrays for repeated use during the simulation of the dynamic process.

As with many relaxation programs this one breaks into violent temporal oscillation if time steps are too long. We do an approximate computation of the shortest period of oscillation or decay of any director if it is displaced while its two nearest neighbours are fixed. If we make the time steps shorter than this period divided by 2π we avoid the problem of oscillations.

RESULTS OF DYNAMIC SIMULATIONS

We have seen no measurements of the five viscosity parameters for E7. The viscosities of MBBA have been determined with fair accuracy. When we used those values in computations we obtained 'rise-times' from the DOWN state to the UP state in our bistable cells that were about half the observed time (Heffner & Berreman 1982). For lack of better information we shall assume that the viscosities of E7 are twice those for MBBA (see table 1). The numbers are not really in the right proportion because observed 'fall-times' from the UP state to the DOWN state are not

quite as slow as these viscosities predict. Accurate values for five separate viscosities for the commonly used nematic mixtures would be very useful.

The possibility of simulating nematic fluid dynamics should allow for the design of simpler experiments to measure viscosities. The program we use allows one surface of the cell to move with respect to the other. With simulation to help in the interpretation, experimental cells with shear may be used to determine various combinations of viscosity parameters, depending on the orientation of the liquid crystal directors at the surfaces.

Even without accurate values for viscosity parameters it is instructive to follow a simulated cycle in a bistable twist cell. This is done in figures 9 and 10. The minimum time that the applied field must be held at a value other than the 'holding voltage' to cause a transition from one bistable state to another is just the time required for the configuration to pass beyond a configuration similar to the unstable equilibrium state between the two stable ones. From that time on, the elastic torques will carry the cell to equilibrium. However, by increasing the switching pulse times slightly, though not too much, the configuration will reach equilibrium in a minimum time because the state at the end of the pulse will closely resemble the intended equilibrium state. Such optimum times were used in figures 9 and 10.

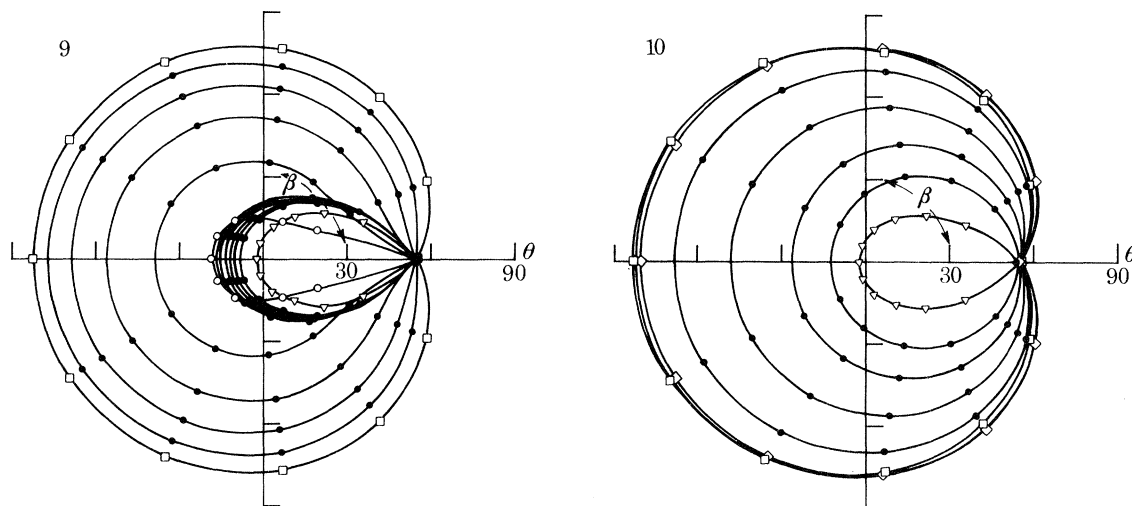


FIGURE 9. Dynamic progression from the equilibrium DOWN state of figure 2 (\square), when thrice 1.86 V (5.62 V) is applied suddenly and continued for 0.01 s, after which the field reverts to 1.86 V. Successive configurations are 0.002 s apart with additional field on, 0.01 s apart with additional field off. Final configuration (∇) is near equilibrium UP state after 0.2 s. Viscosities are twice those for MBBA to give observed transition speed. The cell is 10 μm thick.

FIGURE 10. Progression from preceding UP configuration at 1.86 V (∇) after suddenly switching the field off for 0.1 s and then returning to 1.86 V. Successive configurations are 0.02 s apart. The measured 'down' transition is faster than computed with these viscosities.

Another use of the dynamics program has been to explain the movement of foreign particulate matter and disclinations to the edges of picture elements in ordinary twist cells (Berreman & Sussman 1979). Simulation of laminar flow shows a net movement of fluid across a picture element after repeated cycling. This will result in slower circulation around the element. Particles and disclinations that are weakly attached to the surface appear to be dislodged by the faster flow in the element and lodged at its downstream boundary.

An unexpected result of the simulation of flow in twist cells appears in the explanation of

recent experiments of Hubbard & Bos (1981). They show that cells with a total twist of $\frac{3}{4}$ turn containing chiral nematics are fast and have reduced optical bounce. This result might seem to contradict previous indications that chirality slows the response of twist cells. However, Hubbard & Bos find that the same backflow effect that hinders return to the field-free configuration in $\frac{1}{4}$ turn cells, as indicated by van Doorn (1975) and Berreman (1975*a*), speeds that return in $\frac{3}{4}$ turn cells.

OPTICAL COMPUTATIONS

The 4×4 matrix method of optical computations has been adequately described by Smith (1965) and Berreman & Scheffer (1970). The method has been used in conjunction with a fluid dynamic program to show the complicated variations in twist-cell contrast with both time and viewing direction (Berreman 1975*b*). It has also been used to find optimal relations between cell thickness and optical anisotropy (Baur 1980, 1981; van Doorn *et al.* 1980; Birecki & Kahn 1980). Finally, we observe that in bistable twist cells the contrast is positive in some directions and negative in others. An example of this is shown in figure 11. As with ordinary twist cells, computer simulation has helped us to enhance the contrast and to understand how to improve the range of viewing directions.

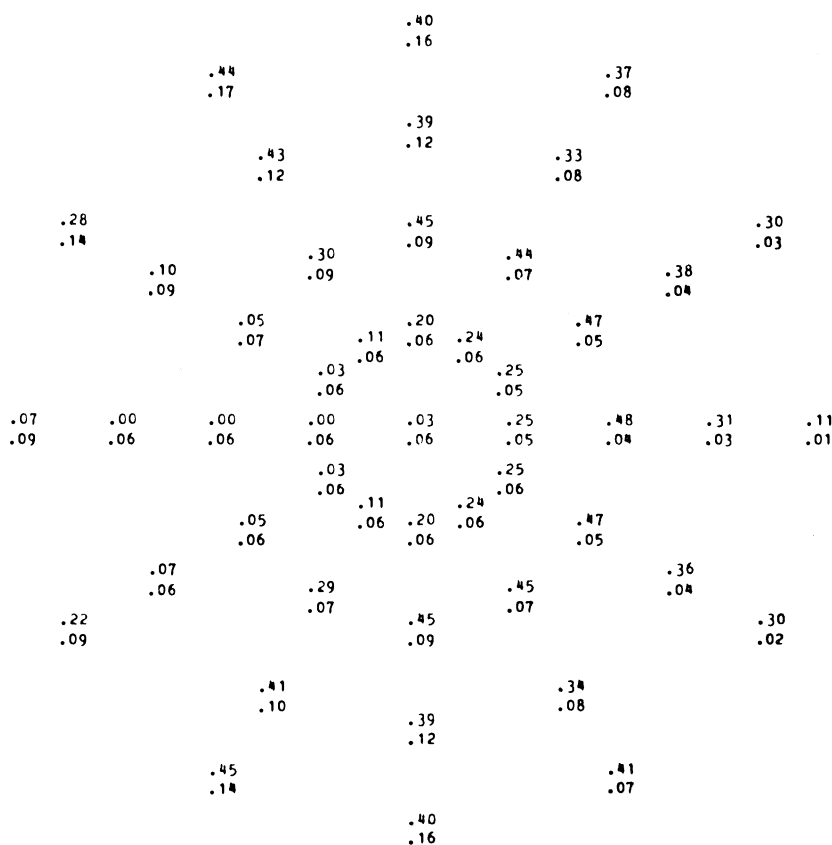


FIGURE 11. Transmission of plane-polarized light by cell similar to that of figure 6 but $16 \mu\text{m}$ thick, in DOWN (bottom numbers) and UP (top numbers) states, when viewed through a perfect crossed polarizer. Angles of view are normal and 10° , 20° , 30° and 40° from normal at 30° azimuth intervals. A region of negative contrast in one quadrant is characteristic of this cell, but it can be reduced in size and moved by altering parameters.

MODELLING IN MORE DIMENSIONS

The modelling alluded to so far is one-dimensional in the sense that director orientation is presumed to vary only along the z direction, normal to the cell surfaces. There are numerous problems that might be better understood through the simulation of configurations that vary in at least two dimensions. For example, lateral instabilities often occur in bistable or highly multiplexed twist cells in experimental stages of development. Greubel discovered this when he attempted to make a bistable, disclination-free chiral nematic twist cell with homeotropic boundary orientation (Greubel 1974). He then described a bistable cell with one state disordered by the instability.

Lateral variations of director configuration are crucial to ‘dynamic-scattering’ cells. Two- or three-dimensional simulation would also lead to better understanding of the fluid behaviour in such scattering cells.

In addition to lateral instabilities, there is the problem of lateral variation of director orientation and flow at the edges of picture elements in every twist cell. The effect of edges on static configurations is rather short-range; being on the order of the cell thickness. However, dynamic effects probably extend over larger distances.

Unfortunately even the analysis of two-dimensional variations is in a very rudimentary state of development. Analytic methods will probably always be restricted to small perturbations from laminar configurations unless inequalities in elastic constants are ignored. The complexity of boundary conditions necessitates the use of relaxation methods in computer simulation. So far, such computer simulations have only been used to find static configurations in the absence of fields (Berreman 1979). Electric field patterns would have to be adjusted after each change in director configuration unless the dielectric anisotropy is assumed to be too small to affect the pattern significantly.

Three-dimensional solutions have been studied even less. However, Sammon (1982) and Meiboom *et al.* (1983) have recently obtained static configurations that may simulate cholesterics in cubic ‘blue phases’ in the absence of fields. They used a fast relaxation method on a high-speed computer, but precision was low for reasonable running times.

The optics of liquid crystals with two- or three-dimensional variations in director is extremely complicated except in certain cases where ray optics or approximate scattering theories can be used. Fortunately, few cases have arisen where more detailed analysis seems necessary.

CONCLUSIONS

Despite present limitations to one dimension, numerical modelling has been very useful in understanding and optimizing the design of nematic and chiral nematic twist cells. If modelling were implemented in two or three dimensions with electric fields it would be possible to study many other important problems. Among these are stability against transverse distortions, movement of configuration walls and the effects of boundaries on flow.

I wish to acknowledge the hospitality and suggestions of the liquid crystal group at the Institut für Angewandte Festkörperphysik in Freiburg i.Br. during some of the development of the computer programs used in this work.

REFERENCES

- Aslaksen, E. W. 1971 *Physik kondens. Materie* **14**, 80.
- Baur, G. 1980 In *The physics and chemistry of liquid crystal devices* (ed. G. Sprokel), pp. 61–78. New York: Plenum Press.
- Baur, G. 1981 *Molec. Cryst. liq. Cryst.* **63**, 45.
- Baur, G., Windscheid, F. & Berreman, D. W. 1975 *Appl. Phys.* **8**, 101.
- Berreman, D. W. 1975a *J. appl. Phys.* **46**, 3746.
- Berreman, D. W. 1975b In *Nonemissive electrooptic displays* (ed. A. R. Kmetz & F. K. Von Willisen), pp. 9–24. New York: Plenum Press.
- Berreman, D. W. 1979 *J. Phys., Paris* **40** (suppl. 4), c3-58.
- Berreman, D. W. 1980 In *The physics and chemistry of liquid crystal devices* (ed. G. Sprokel), pp. 1–13. New York: Plenum Press.
- Berreman, D. W. & Heffner, W. R. 1982 In *S.I.D. Int. Symp. Digest Tech. Papers*, vol. 13, p. 242.
- Berreman, D. W. & Scheffer, T. J. 1970 *Molec. Cryst. liq. Cryst.* **11**, 395.
- Berreman, D. W. & Sussman, A. 1979 *J. appl. Phys.* **50**, 8016.
- Birecki, H. & Kahn, F. J. 1980 In *The physics and chemistry of liquid crystal devices* (ed. G. Sprokel), pp. 125–142. New York: Plenum Press.
- de Gennes, P. G. 1975 *The physics of liquid crystals*, equation 6.43. Oxford University Press.
- de Jeu, W. H. 1978 *Phys. Lett. A* **69**, 122.
- Deuling, H. J. 1974 *Molec. Cryst. liq. Cryst.* **27**, 81.
- Ericksen, J. L. 1961 *Trans. Soc. Rheol.* **5**, 23.
- Frank, F. C. 1958 *Discuss. Faraday Soc.* **25**, 19.
- Goldstein, H. 1950 *Classical mechanics*, chapter 1. Addison-Wesley Press.
- Greubel, W. 1974 *Appl. Phys. Lett.* **25**, 5.
- Heffner, W. R. & Berreman, D. W. 1982 *J. appl. Phys.* **53**, 8599.
- Hubbard, R. L. & Bos, P. J. 1981 *IEEE Trans. Electron. Devices* **ED-28**, 723.
- Leslie, F. M. 1968 *Arch. ration. Mech. Analysis* **28**, 265.
- Leslie, F. M. 1970 *Molec. Cryst. liq. Cryst.* **12**, 57.
- Meiboom, S., Sammon, M. & Brinkman, W. F. 1983 *Phys. Rev. A* **27**, 438.
- Oseen, C. W. 1933 *Trans. Faraday Soc.* **29**, 883.
- Raynes, E. P., Tough, R. J. A. & Davies, K. A. 1979 *Molec. Cryst. liq. Cryst. Lett.* **56**, 63.
- Sammon, M. J. 1982 *Molec. Cryst. liq. Cryst.* **89**, 305.
- Scheffer, T. J. 1980 In *Advances in liquid crystal research and applications* (ed. L. Bata), pp. 1145–1153. Oxford: Pergamon Press.
- Smith, D. O. 1965 *Optica Acta* **12**, 13.
- Thurston, R. N. 1982 *J. Phys., Paris* **43**, 117.
- Thurston, R. N. & Berreman, D. W. 1981 *J. appl. Phys.* **52**, 508.
- van Doorn, C. Z. 1975 *J. appl. Phys.* **46**, 3738.
- van Doorn, C. Z., Gerritsma, C. J. & de Klerk, J. J. 1980 In *The physics and chemistry of liquid crystal devices* (ed. G. Sprokel), pp. 95–104. New York: Plenum Press.
- Yang, K. H. 1982 *J. appl. Phys.* **53**, 6742.